

On the Influence of Graphite Electrodes in Sinking EDM of Ti6Al4V Alloy

Armorim, F.; Torres, R; Soares, P. C.; Laurindo, C.

Abstract. Titanium alloys have an increasing application in industrial environment due to their excellent properties of high resistance to corrosion, resistance to high temperatures, low specific density and mechanical strength similar to steel. These characteristics make titanium alloys widely used in the aerospace and biomedical fields. However, titanium and its alloys have high chemical reactivity with most of the cutting tools. It marks these alloys as difficult to be worked by conventional machining processes. Electrical Discharge Machining (EDM) emerges as an alternative to machining of these materials. This work investigated the performance of special grades of graphite as electrodes when EDMing Ti6Al4V under three different regimes. The main influences of electrical parameters are discussed for material removal rate, volumetric relative wear and roughness. This work contributes with an understanding of economic conditions for EDMing of Ti6Al4V alloy using special graphite electrodes.

NOMENCLATURE

τ – duty factor (t_i / t_p) [μs]

ϑ – volumetric relative wear (V_e / V_w) [%]

\hat{u}_i – open circuit voltage [V]

t_e – average discharge voltage [V]

t_d – ignition delay time [μs]

t_e – discharge duration [μs]

t_i – pulse duration ($t_d + t_e$) [μs]

t_0 – pulse break time [μs];

t_p – pulse cycle time ($t_i + t_0$) [μs]

i_e – discharge current [A];

V_w – material removal rate [mm^3/min]

V_e – electrode wear rate [mm^3/min]

W_e – discharge energy ($\bar{u}_e \cdot i_e \cdot t_e$) [J]

1 INTRODUCTION

Titanium alloys are widely used for aerospace components, medical and dentistry implants and instruments, power generation and chemical processing applications among other industrial fields. This extensive usage is related to the properties of low density, very high strength-to-weight ratio, high temperature and corrosion resistance, as well as biocompatibility. Compared to other special alloys, titanium alloys have much more applications in the industry as pointed out by Gu *et al.* (2012).

However, titanium and its alloys are very expensive when compared to other materials for the same applications. In part, this is due to several factors, as for instance the complexity of extraction process, difficulty of melting and problems related to the production of raw industrial shapes as remarked by Suzuki *et al.* 1999. Some other constraints are related to machining and other manufacturing processes. Near-net-shape manufacturing processes (e.g. isothermal forging and powder metallurgy) were introduced to reduce manufacturing costs of titanium components. Nevertheless, most titanium alloy parts for several applications are produced by conventional machining processes: drilling, milling, turning and grinding as previously reported by Ezugwu and Wang (1997).

Ezugwu *et al.* (2003) reported that titanium alloys are usually considered as a difficult-to-machine material due to several titanium alloys characteristics. They remark some common failure manners as being notching at the tool nose, flank and crater wear, chipping and catastrophic cutting tool failure. The low thermal conductivity of the titanium increases considerably the temperature at the part/cutting tool interface, which weakens the cutting edge reducing the tool life. It makes the majority of commercially cutting tools to be used only at moderate cutting speed conditions (Wang *et al.* 2005). Titanium is also chemically reactive with the most cutting tools, which facilitates the adhesion of material on the tool during machining, promoting accelerated tool wear. Furthermore, the high strength and low elasticity modulus of titanium alloys at high temperatures promote the welding of the workpiece to the tool cutting edge, which forms unstable built-up edge deteriorating the machined surfaces and worsening the components surface integrity as presented by Hartung *et al.* (1982).

Superior cutting tool materials as for example CBN and PCBN have been used to produce high quality parts at higher cutting speeds (Zoya and Krishnamurthy, 2000) as well as polycrystalline diamond (Oosthuizen *et al.* 2011). Other special techniques such as ramping or taper turning and rotary machining together with the application

of high pressure coolant, cryogenic cooling and minimum quantity of cooling lubricant (MQL) have been explored by researchers (Ezugwu *et al.* 2003), but all of them presenting limited success (Gu *et al.*, 2012). Alternatively, non-conventional machining processes can be used as different methods to improve the machining performance of the titanium alloys, where among these emerges the electrical discharge machining (Kibria *et al.*, 2010).

The electrical discharge machining (EDM) is a non-conventional machining process that uses the conversion of electrical energy into thermal energy to remove material from the workpiece. The EDM efficiency depends fundamentally on the thermophysical properties of the electrode tool and the workpiece to be machined. Thus, the erodibility of a material shows very little dependence of its mechanical properties, as opposed to conventional machining techniques. As presented by Abbas *et al.* (2007) and Ho and Newman (2003), the EDM process have been applied in the machining of ferrous and non-ferrous alloys, electrical conductive ceramic materials, composite materials and special alloys. They also remark that nowadays the main areas of EDM research worldwide are still related to topics such as process performance parameters, process control and monitoring techniques and workpiece surface integrity, among others. Hasçhk e Çaydas (2007) highlight that there is a relatively lack of research in EDM of titanium alloys concerning parameter settings optimization for different electrode materials as well as studies on aspects of surface integrity characteristics. Lately, Gu *et al.* (2012) also remarked that efficient and economical machining of titanium alloys continues to attract the interest of industry and academia researchers.

Based on the aforementioned arguments, the present work investigated the influence of EDM electrical parameters when machining Ti6Al4V alloy using three special grades of graphite as electrode material under different regimes. The process performance was evaluated and discussed for material removal rate, volumetric relative wear and roughness. This work contributes with an understanding of economic conditions for ED-Machining of Ti6Al4V alloy using special graphite electrodes.

2 SOME THEORETICAL EDM BACKGROUND

This section presents information related to EDM material removal mechanism in order to enlarge the understanding of the experimental methodology proposed in this study and discussion of the results achieved. From investigations of DiBitonto *et al.* (1989), Mukund *et al.* (1989), Eubank *et al.* (1993), König & Klocke (1997), Kunieda *et al.* (2005), and many other researchers, the material removal in electrical

discharge machining is associated with the erosive effect produced when spatially and discrete discharges occur between two electrical conductive materials. Sparks of short duration, ranging from 0,1 to 4000 μs , are generated in a liquid dielectric working gap separating the electrode and the workpiece (10-1000 μm). The discharge energy $W_e \approx u_e \cdot i_e \cdot t_e$ [J] released by the generator is responsible to melt a small quantity of material of both electrode and workpiece by conduction heat transfer. Subsequently, at the end of the pulse duration, a pause time begins and the melted pools are removed by forces which can be of electric, hydrodynamic, thermodynamic and spalling nature.

Figure 1 (A) briefly presents the phases of a discharge in EDM process and Fig.1 (B) shows the concept of EDM. The first phase is the ignition phase which represents the lapse corresponding to the occurrence of the breakdown of the high open circuit voltage \hat{u}_i applied across the working gap until the fairly low discharge voltage u_e , which normally ranges from 10 to 40 V. This period is known as ignition delay time t_d [μs]. The second phase, which instantaneously occurs right after the first one, when the current rapidly increases to the discharge current \hat{i}_e [A], is the formation of a channel of plasma surrounded by a vapor bubble. The third phase is the discharge phase, when the channel of plasma of high energy and pressure is sustained for a period of time t_e [μs] causing melting and evaporation of small amounts of material in both electrode and workpiece. The fourth, and last one phase, is the collapse of the channel of plasma caused by turning off the electric energy, which causes the molten material to be violently ejected. At this time, known as interval time t_o [μs], a part of the molten and vaporized material is flushed away by the flow of the dielectric fluid across the gap and the rest is solidified in the recently formed crater and surroundings. During the interval time t_o also occurs cooling of electrode/workpiece and de-ionization of the working gap, necessary to promote an adequate dispersion of successive discharges along the surfaces of the electrode and the workpiece. This process continues until the geometry of the part is completed. Considering the aforementioned EDM phenomenon an asymmetric material removal of the electrode and the workpiece can be achieved by the appropriate choice of electrical parameters, electrode polarity, type of working gap flushing, planetary movement of the electrode and thermophysical properties of electrode/workpiece materials.

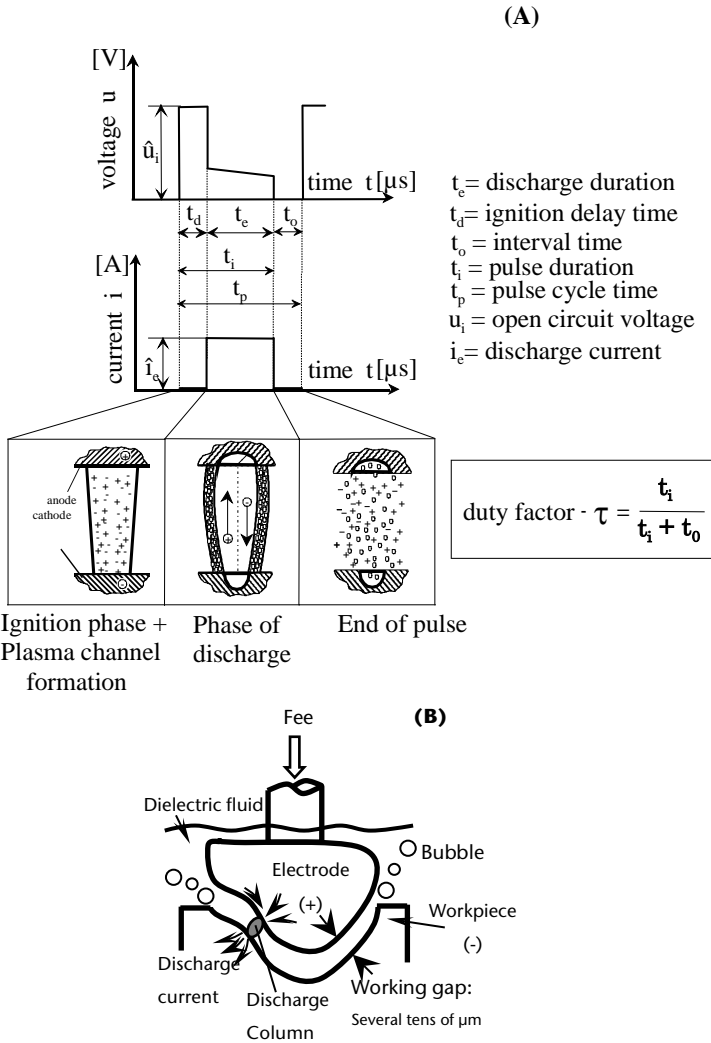


Figure 1: (A) Schematic representation of the phases of an electric discharge in EDM and the definition of duty factor τ and (B) the concept of EDM phenomenon.

According to Amorim & Weingaertner (2002) another EDM variable strictly associated to the electrical parameters and that influences on the machining characteristics is the duty factor τ , illustrated in Fig.1.

The duty factor can affect the material removal rate V_w , the volumetric relative wear \mathcal{G} and the workpiece surface roughness R_a . The duty factor τ is the ratio between the pulse duration t_i and the pulse cycle time t_p ($t_i + t_o$). The value of duty factor τ should be chosen as high as possible. The usual procedure to increase the value of τ is by reducing the pulse interval time t_o and keeping the pulse duration t_i constant. This procedure leads to the increase of discharge frequencies promoting better rates of V_w and lower values of \mathcal{G} . An important aspect regarding the choice of high values of τ is associated with the elevation of the contamination concentrated in the working gap. According to Schumacher (1990) some concentration of sub-microscopic particles, fibers or moisture drops in the working gap can reduce the ignition delay time t_d . It happens because these particles arrange themselves in such a way that a kind of a bridge occurs intensifying the electric field. This then quickly fires another discharge. On the other hand very high values of duty factor τ is responsible to promote many short-circuits and arc-discharges causing low values of V_w and high levels of \mathcal{G} . In current practice of EDM of metal alloys conservative decisions are taken to gain safer machining performance. This means the use of duty factor $\tau = 0,5$ ($t_i = t_o$) in order to avoid short-circuit, arc-discharges and good flushing conditions. For duty factor higher than 0,5 ($t_i > t_o$) the machining conditions might become worse and arcing damages can occur. Values of duty factor lower than 0,5 ($t_i < t_o$) lead to low machining rate. In the present work the duty factor of $\tau = 0,5$ was then used.

3 EXPERIMENTAL METHOD AND PROCEDURES

Figure 2 shows the schematic methodology designed for the experiments followed by the materials and equipment.

(i) EDM machine: a Charmilles ROBOFORM 30 CNC machine equipped with an isoenergetic generator, which means that it is possible to set the energy W_e supplied to the working gap during a spark ($W_e = u_e \cdot i_e \cdot t_e$ [mJ]), was employed.

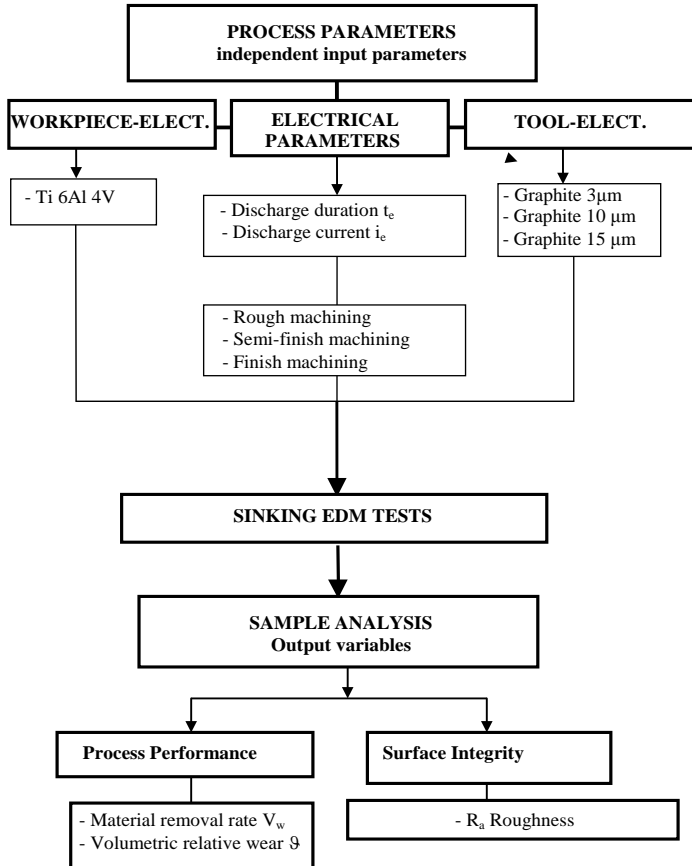


Figure 2: Schematic methodology for the experiments, presenting input variables and output EDM performance variables evaluated.

(ii) *Tool-electrode*: cylindrical bars of 3 special grades of graphite (Tab. 1), manufactured by SGL Carbon Group (Germany) were used. Electrodes were machined with 20 mm outer diameter and 4 mm central hole for pressure flushing. The electrodes were mounted axially in line with the workpiece samples. A hydrocarbon dielectric fluid with viscosity at 40°C of 3 cSt, flash point of 125°C, density of

0,783 g/ml and 0,3% of aromates was injected through the central hole with pressure of 0.01 MPa.

Table 1: Physical and mechanical properties of the special graphite (thin, super-thin and ultra-thin).

Particle size	µm	15	10	3
Classification		Thin	Super-thin	Ultra-thin
Density	g/cm ³	1.72	1.77	1.88
Open porosity	%	15	13	10
Pore diameter	µm	2	1.5	0.6
Permeability	X10 ⁻² cm ² /seg	15	10	1
Hardness		80 HR10/100	70 HR5/100	110 HR5/100
Bending strenght	N/mm ²	45	50	85
Elasticity	kN/mm ²	10.5	10.5	13.5
Resistivity	µΩm	12	14	13
Thermal conductivity	Wm ⁻¹ K ⁻¹	90	80	100
Thermal expansion	X10 ⁻⁶ /K	2.9	3.9	4.7
Ash content	ppm	200	200	200

(iii) Workpieces: Specimens of titanium alloy Ti6Al4V (chemical composition: 6% Al, 4% V, 0,3% Fe, 0,2%, 0,10% C, 0,05% N, remainder Ti) with dimensions 25 X 25 15 mm were cut by wire EDM (Charmilles ROBOFIL 290) with a surface roughness of R_a = 1.0 µm. Table 2 presents the physical and mechanical properties of the samples.

Table 2: Physical and mechanical properties of Ti6Al4V.

Density	g/cm ³	4.42
Melting point	°C	1649
Specific heat	J/Kg. °C	560
Electric resistivity	Ohm.cm	170
Thermal conductivity	W/m.K	7.2
Yield strength	MPa	897 – 1000
Modulus of elasticity	GPa	114
Hardness	HR _C	36

(iv) Electrical EDM parameter settings: Three regimens of machining for roughing, semi-finish and finish were carried out as shown in Tab.3. For each test condition three repetitions were applied and no significant changes in performance were observed. The duty factor τ was maintained at 0,5 to provide adequate flushing of debris away from the working gap. The electrodes were negatively charged for the main experiments, because during the pilot tests with positive electrodes it was observed low workpiece material removal due to formation of oxidized layers on the surface of Ti6Al4V workpiece samples. A 45 min machining time for each regime were applied in order to properly quantify the material removal rate V_w [mm³/min] and the volumetric relative wear $\mathcal{Q}(V_e / V_w)$ [%].

Table 3: Electrical variables used for the EDM experiments.

Regime	i_e [A]	Graphite particle size [μm]	t_e [μs]	t_0 [μs]	\hat{u}_i [V]	Electrode polarity
Finish	3	3; 10; 15	6,4; 12,8; 25; 50; 100	6,4; 12,8; 25; 50; 100	160	Negative
Semi-finish	12	3; 10; 15	6,4; 12,8; 25; 50; 100	6,4; 12,8; 25; 50; 100	120	Negative
Rough	32	3; 10; 15	12,8; 25; 50; 100; 200	12,8; 25; 50; 100; 200	80	Negative

The precise quantification of the material removal rate V_w and volumetric relative wear ϑ was possible using a precise scale (resolution of 0,0001 g) to weigh the electrode and workpiece samples before and after each EDM experiment. It is important to mention that during the EDM process the graphite electrodes can absorb some quantity of the dielectric fluid because of their porosity. A drying period was carried out to minimize any error when measuring the electrodes masses. As for that, the electrodes were kept in a furnace at 150°C for 24 hours before and after each EDM experiment. By using the density of the materials, the volume of the material removed was accurately calculated.

4 RESULTS AND DISCUSSION

The results of material removal rate V_w against the variation of discharge duration t_c for finishing, semi-finishing and roughing regimes using thin [15 μm], super-thin [10 μm] and ultra-thin [3 μm] graphite electrode's particles sizes are summarized in Fig.3. It shows that the graphite electrode with 10 μm particle size provided the best values of material removal rate V_w for all regimes. A possible explanation lies in the fact that increasing the graphite particle size from 3 to 10 μm increases the detachment of tiny graphite particles from the electrode by spalling effect, right after the plasma channel collapse. These particles then collide into the melted pool on the workpiece, assisting the ejection of melted material after the energy is turned off and the dielectric fluid flushes the debris away from the working gap.

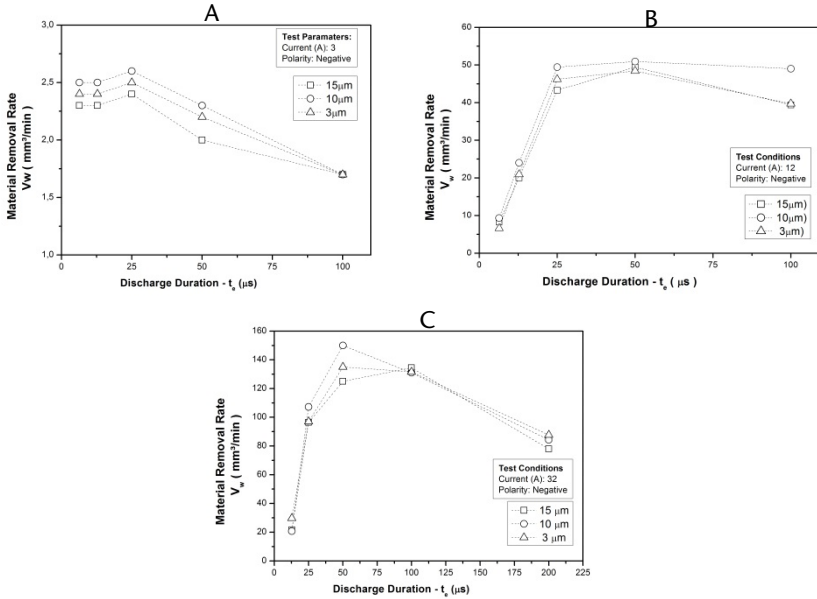


Figure 3: Results of material removal rate V_w for three particle sizes of graphite under EDM regimes: (A) finishing, (B) semi-finishing and (C) roughing.

The increase of graphite particle sizes from 10 to 15 μm does not cause improvement of material removal rate V_w , but instead it lowers the V_w attained. It might be suggested to spalling detachment of grosser tiny particles at excessive amounts that obstruct the working gap and hinders the flushing of debris away. It then promotes overcontamination of the gap, which ends up forming arcing and short circuits, decreasing the values of V_w as can be seen in Fig. 3 regardless the discharge current i_e applied (3, 12, 32 A).

Additionally, it can be noticed from Fig.3 that, no matter the particle size of the graphite electrode, as the discharge duration t_e increases, regardless the value of discharge current i_e , the rate V_w also increases up to a maximum value for a specific optimum t_e . The highest material removal rate V_w is approximately of 150 mm³/min for $i_e = 32$ A to the optimum $t_e = 50$ μs using the 10 μm graphite particle size. After this point V_w starts to decrease. It arises from longer discharge duration t_e that diminishes the pressure and energy of the plasma channel

over the molten material of the electrode and the workpiece. As a consequence, process instability in the form of short circuits and arc-discharges takes place lowering the material removal rate V_w . This behavior is also observed for the other current discharges applied ($i_e = 3$ and 12 A) using 15 and 3 μm graphite particle sizes, where the maximum values of V_w were for $t_e = 25$ μs .

It is noteworthy that a black film on the surface of the samples was observed for the experiments with graphite electrodes of $15\mu\text{m}$ for any value of discharge duration t_e and discharge current i_e . This is likely to be due to grosser graphite particles detached from the electrode, which was not properly evacuated out of the gap. These particles then deposited over Ti6Al4V workpiece surface.

The volumetric relative wear ϑ represents the ratio between the electrode wear rate V_e [mm^3/min] to the workpiece material removal rate V_w [mm^3/min]. The results of ϑ [%] as a function of discharge duration t_e for currents $i_e = 3$, 12 and 32 A are shown in Fig. 4. The lowest value of ϑ of about 15% was reached for 32 A ($t_e = 50$ μs) employing 3 μm graphite particle size, a little lower than that for 10 μm graphite electrode. When ED-Machining with discharge current $i_e = 3$ and 12 A the values of ϑ were respectively around 60% and 23% for the optimum discharge duration $t_e = 25$ μs . It is important to remark that for discharge durations t_e higher than the optimum values the volumetric relative ϑ (V_e/V_w) increases. This is induced by the decrease of the material removal from the workpiece owing to longer discharge duration t_e . For values of t_e higher than the optimum the forces generated by the plasma channel collapse is not enough to properly expulse the debris, which afterwards end up solidifying on the recently formed crater and surroundings.

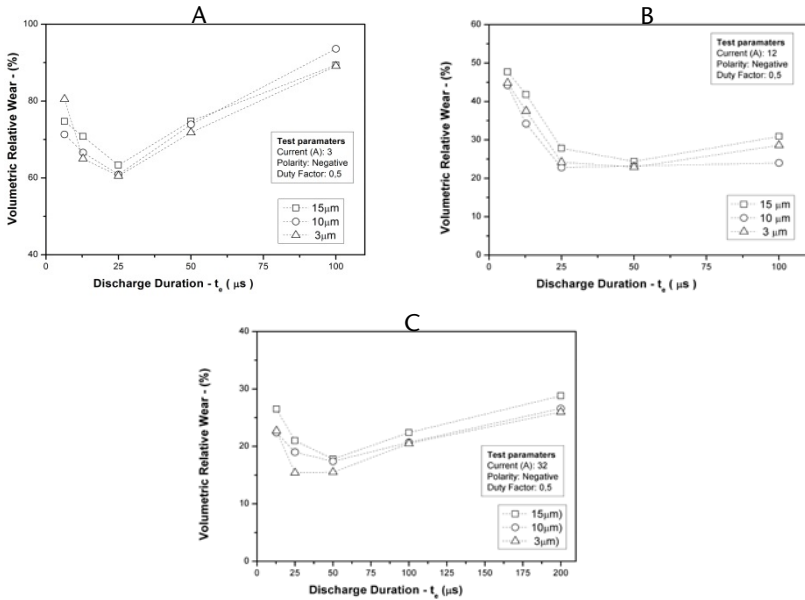


Figure 4: Results of volumetric relative wear η [%] for three particle sizes of graphite under EDM regimes: (A) finishing, (B) semi-finishing and (C) roughing.

Figure 5 depicts the surface roughness R_a for finishing ED-Machining conditions. It can be clearly seen the best R_a around $2,2 \mu\text{m}$ achieved for 3 and $10 \mu\text{m}$ graphite electrodes' particle sizes at $6,4 \mu\text{s}$ discharge duration t_e , which is better than that ($R_a = 3,1 \mu\text{m}$) for the optimum $t_e = 25 \mu\text{s}$. It possibly lies on the increase of energy ($W_e \approx u_e \cdot i_e \cdot t_e$), delivered to the plasma channel, that melts more material producing larger and deeper craters on the surface up to the optimum discharge duration t_e . Beyond such t_e the plasma channel becomes unstable, promoting reduction of material removal rate because the molten material is not adequately ejected and flushed from the gap. The larger and non-uniform debris are then laid on the surface increasing the roughness (e.g. from $t_e = 25 \mu\text{s}$ to $100 \mu\text{s}$).

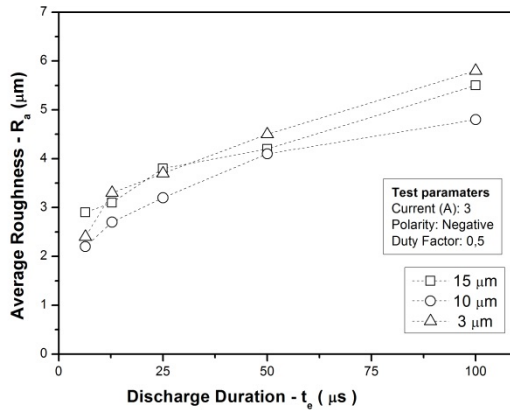


Figure 5: Surface Roughness R_a for finishing ED-Machining ($i_e = 3$ A) using thin [15 μm], super-thin [10 μm] and ultra-thin [3 μm] graphite electrode's particles sizes.

5 CONCLUSIONS

The present work investigated the influence of EDM electrical parameters when machining Ti6Al4V alloy using three special grades of graphite as electrode material under different regimes. The best results for material removal rate and volumetric relative wear were obtained with the graphite electrode of 10 μm particle size and negative polarity. The use of a positive electrode, despite the graphite particle size, promoted very low material removal rate due to formation of oxides on the Ti6Al4V workpiece samples, which inhibited the breakdown of open circuit voltage. A black film adhered on the workpiece surface was observed when using 15 μm graphite electrode for all the EDM regimes experimented. The best value of roughness R_a approximately 2,2 μm was obtained for machining with the graphite electrode of 10 μm particle size with discharge duration $t_e = 6,4$ μs and discharge current $i_e = 3$ A. The price for graphite material raises considerably as the particle sizes diminishes. Regardless the ED-Machining regime (rough, semi-finish and finishing) and the graphite particle size (15, 10 and 3 μm) an adequate cost-benefit ratio for ED-Machining of Ti6Al4V is the use of 10 μm graphite.

6 REFERENCES

- /1/ Abbas, N. M., Solomon, D. G. and Bahari, M. F., 2007, "A review on current research trends in electrical discharge machining (EDM)", *International Journal of Machining Tools and Manufacture*. Vol. 47, p. 1214-1228.
- /2/ Amorim, F. L., Weingaertner, W. L., 2002, "Influence of Duty Factor on the Die-Sinking Electrical Discharge Machining of High-Strength Aluminum Alloy under Rough Machining", *Journal of the Brazilian Society of Mechanical Sciences*, Vol. 24, p. 194-199.
- /3/ DiBitonto, D. D., Eubank, P. T., Patel, M. R. and Barrufet, M.A., 1989, "Theoretical models of the electrical discharge machining process I: a simple cathode erosion model", *Journal of Applied Physics*, Vol. 66 9, p. 4095-4103.
- /4/ Eubank, P. T., Patel, M. R., Barrufet, M.A. and Bozkurt, B., 1993, "Theoretical models of the electrical discharge machining process III: the variable mass, cylindrical plasma model", *Journal of Applied Physics*, Vol. 73 11, p. 7900-7909.
- /5/ Ezugwu, E.O., Bonney, J., Yaman, Y., 2003. "An overview of the machinability of aeroengine alloys". *Journals of materials processing technology*. Vol. 134, p. 233-253.
- /6/ Ezugwu, E.O., Wang, Z.M., 1997. "Titanium alloys and their Machinability". *Journal of Materials Processing Technology*. Vol. 68, p.262-274.
- /7/ Gu, L., Lei, L., Zhao, W., Rajurkar, K.P., 2012. "Electrical discharge machining of Ti6Al4V with a bundled electrode". *International Journal of Machine Tools and Manufacture*. Vol. 53, p.100-106.
- /8/ Hartung, P.D., Kramer, B.M., 1982. "Tool wear in titanium machining". *CIRP Annals – Manufacturing Technology*. Vol. 31, p.75-80.
- /9/ Haçhk, A., Çaydas, U., 2007, "Electrical discharge machining of titanium alloy (Ti-6Al-4V)", *Applied surface science*, Vol. 253 22, p. 9007-9016.
- /10/ Ho, K. H. and Newman, S.T., 2003. "State of the art electrical discharge machining (EDM)". *International Journal of Machine Tools & Manufacture*. Vol. 43, p. 1287-1300.

- /11/ Kibria, G. Sarkar, B.R., Pradhan. B.B., 2010. "Comparative study of different dielectrics for micro-EDM performance during micro hole machining of Ti-6Al-4V alloy". *International Journal of Advanced Manufacturing Technology*. Vol. 48, p.557-570.
- /12/ König, W. and Klocke, F., 1997, "Fertigungsverfahren - 3: Abtragen und Generieren", Berlin, Springer, Vol. 3.
- /13/ Kunieda, M., Lauwers, B., Rajurkar, K.P. Schumacher, B.M., 2005, "Advancing EDM through fundamental insight into the process", *Annals of CIRP Manufacturing Technology*, Vol. 54 2, p.599-622.
- /14/ Mukund, R., Patel, M.A.B., Eubank, P.T. 1989, "Theoretical models of the electrical discharge machining process II: the anode erosion model", *Journal of Applied Physics*, Vol. 66 9, p. 4104-4111.
- /15/ Oosthuizen, G.A., Akdogan, G., Treurnicht, N., 2011. "The performance of PCD tools in high-speed milling of Ti6Al4V". *International Journal of Advanced Manufacturing Technology*. Vol. 42 9-12, p. 929-935.
- /16/ Schumacher, B. M. 1990. "About de role of debris in the gap during electrical discharge machining". *Annals of the CIRP Manufacturing Technology*. Vol. 39 1, p.197-190.
- /17/ Suzuki, H.G., Takakura, E., Eylon, D., 1999. "Hot strength and hot ductility of titanium alloys – a challenge for continuous casting process". *Materials Science and Engineering*. Vol. A263, p. 230-236.
- /18/ Wang., Z.G., Wong, Y.S., Rahman, M. 2005. "High-speed milling of titanium alloys using binderless CBN tools". *International journal of Maching Tools and Manufacture*. Vol. 45, p. 105-114.
- /19/ Zoya, Z.A., Krishnamurthy, R. 2000. "The performance of CBN tools in the machining of titanium alloys". *Journal of Materials Processing Technology*. Vol. 100 1-3, p. 80-86.